Multilayer Platform for Ultra-Low-Loss Waveguide Applications

Demis D. John, Martijn J. R. Heck, Jared F. Bauters, Renan Moreira, Jonathon S. Barton, John E. Bowers, and Daniel J. Blumenthal

***Abstract*— We investigate a multilayer vertical stacking scheme for use in the Silicon Nitride-based low-loss waveguide platform. In this letter, we use common fabrication techniques to produce test structures for probing the interactions between vertically separated parallel waveguide planes and the characteristics of vertical directional couplers. Single-mode and multimode waveguide geometries are investigated, with designs similar to our previously demonstrated ultra-low-loss technologies. Group index measurements via narrowband OFDR reveal an index mismatch between the vertically separated waveguides of 8.6E-3, generated by the stress of the deposited upper cladding. Vertical directional couplers with a 3-μm vertical coupling gap and a 50 nm × 4 μm geometry exhibited an excess coupling loss of 0.19 ± 0.20 dB and cross-coupled power of 54%, limited by the aforementioned velocity mismatch. The 1.23-m spiral structures with perpendicular crossings on adjacent layers show a transmission loss of the crossings below 0.25 dB for a multimode geometry, while the single-mode design showed a minimum crossing loss of 1.0 dB.**

***Index Terms*— Directional couplers, optical waveguides, three-dimensional (3-D) photonic-integrated circuits.**

I. Introduction

WE RECENTLY demonstrated record low losses in a Si_3N_4/SiO_2-based planar waveguide technology, allowing for the creation of optical delay line lengths not previously possible on a chip-scale integrated platform [1], [2]. This enables the use of integrated optical waveguides in otherwise unfeasible applications.

Fiber optic gyroscopes (FOGs) are a particularly interesting example, as the interferometric variety require long optical loops, 10's of meters or more, for increased angular sensitivity [3]. These are currently created with optical fiber, which exhibit the necessary low-loss but require management of polarization birefringence and vibrations.

Our previous waveguide delay demonstrations are highly polarization-maintaining and appear to be well suited for use in FOGs. These designs used Archimedean spirals in which a central "s-bend" reverses the spiral direction. This retrograde spiraling, however, is not compatible with FOG applications, which require that launched light propagate in only one rotational direction. One approach to eliminate retrograde spiraling is to couple light to a second parallel waveguide plane, which would also enable the removal of the tight bend-radius s-bend and consequently enable a longer delay.

Manuscript received November 25, 2011; revised February 22, 2012; accepted February 27, 2012. Date of publication March 5, 2012; date of current version April 20, 2012. This work was supported in part by DARPA MTO under the iPhoD Project under Contract HR0011-09-C-0123.

The authors are with the Department of Electrical and Computer Engineering, University of California, Santa Barbara, CA 93106 USA (e-mail: demis@engineering.ucsb.edu).

Color versions of one or more of the figures in this letter are available online at http://ieeexplore.ieee.org.

Digital Object Identifier 10.1109/LPT.2012.2189762

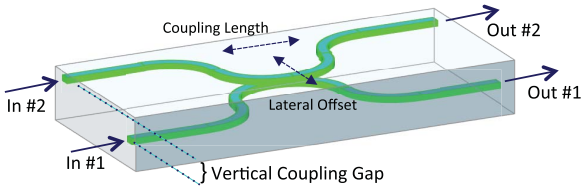

Fig. 1. Schematic of the vertical directional coupler.

Little & Kokubun applied vertically coupled waveguide layers to ring resonators, demonstrating reduced sensitivity to lateral alignment and improved fabrication tolerance due to tight control of layer thicknesses [4], [5].

Thus, in this letter we investigate the feasibility of a multilayer platform on the Si_3N_4/SiO_2 material system. We first study the coupling between parallel waveguides for insight into directional coupler design and inter-layer crosstalk. We additionally investigate perpendicular crossings to probe reflection and scattering losses.

II. Design and Fabrication

Fig. 1 shows a schematic of the vertical directional couplers fabricated, in which the coupling region is designated by a selective vertical overlap area accessed by s-bends with a radius of 9.8 mm. The coupling coefficient of a directional coupler is typically designed via the spacing between waveguides, which in this case is the deposited SiO_2 between waveguide layers, referred to as the *coupling gap*. In the case of vertical couplers we have an additional degree of freedom, the *lateral offset*, to control the coupling coefficient. This is a lithographically defined shift of the overlapping waveguide sections. The *coupling length* is defined as the length of straight waveguide in the overlap region, although there will be some additional mode overlap in the waveguide bends at the entrance and exit of the coupler.

To characterize the coupling between parallel waveguides, an array of vertical couplers with 11 varying coupling lengths and 8 lateral offsets were fabricated. This yields the coupling loss along with other characteristic curves (see section III-B).

To investigate the other extreme of perpendicularly oriented waveguides, 1.23 meter spirals with perpendicular crossings on the vertically separated layer were used to measure the loss & reflection caused by 2nd layer perturbations, as shown in Fig. 2(a). These spirals were measured with the powerful

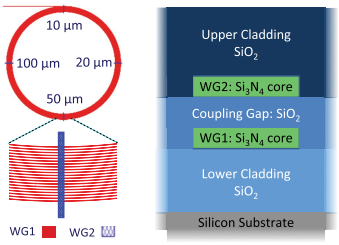

(a) (b)

Fig. 2. (a) Schematic of vertically separated waveguides. (b) Spiral with perpendicular crossings.

OFDR (Optical Frequency-Domain Reflectometry) tool used for loss measurements in our previous work, yielding loss and waveguide-coupled backscatter for each crossing width. Included on each layer are similar spirals without crossings, allowing for correction of the modal index via the OFDR plot.

The waveguide geometries fabricated here are based on the ultra-low loss Silicon Nitride platform shown in [1], in which high aspect ratio geometries were used for both single and multimode guides. For the initial demonstrations in this work we used PECVD (Plasma Enhanced Chemical Vapor Deposition) films and deposited claddings, rather than LPCVD (Low Pressure CVD) and bonded claddings. This leads to higher propagation losses due to increased hydrogen content.

We fabricated Nitride-strip geometries of two widths: 4 μm & 15 μm per device, which are single and multimode, respectively. The film thicknesses & refractive indices are shown in Table I, as measured with multiangle spectroscopic ellipsometry on deposition watch samples. Fig. 2(b) shows a cross-sectional schematic of the vertical coupling scheme and associated thin-films. Thermally grown oxide (on Boron-doped silicon) was used for the lower cladding, with a refractive index of 1.4458 at 1550 nm. PECVD was used to deposit the 1st Si_3N_4 waveguide core (WG1), the Coupling Gap oxide and 2nd Si_3N_4 waveguide core (WG2). For Wafer 1, 50 nm Si_3N_4 cores were deposited, separated by a 3 μm SiO_2 coupling gap. Wafer 2 utilized 60 nm thick waveguide cores with the same coupling gap. Each waveguide core layer was patterned with standard contact lithography and ICP-RIE etching techniques (Reactive Ion Etching with an Inductively Coupled Plasma). 10 μm of SiO_2 upper cladding was deposited with ICP-PECVD for all three samples. Lastly, the wafers were annealed for 3 hours at 900°C for Wafer 1 and 1000°C for Wafer 2. This anneal reduces the PECVD film thickness by about 5%, which was accounted for during the initial depositions to achieve the desired final thicknesses. The thicknesses and refractive indices in Table I reflect those of watch samples after annealing.

TABLE I

MEASUREMENTS OF THIN-FILMS USED IN FABRICATED COUPLERS

	Waveguide Function	Film Thickness	Refractive Index
Wafer 1	WG1 Core	50 nm	1.939
	Coupling Gap	2,952 nm	1.466
	WG2 Core	49 nm	1.940
Wafer 2	WG1 Core	60 nm	1.978
	Coupling Gap	2,923 nm	1.472
	WG2 Core	62 nm	1.985

III. MEASUREMENTS

A. Modal Index Measurements

OFDR measurements of the 1.23 m spirals on either layer of Wafer 2 yielded the optical time-delay between the input facet of the chip and the rectangular termination of the spiral, which was then used to determine the group index (n_g) of each waveguide via knowledge of the lithographically designed spiral length as described in [1]. The 200 μm dicing kerf imparts an error of $\pm 2.32 * 10^{-4}$ to the group index due to the resultant spiral length uncertainty. Using our previously developed narrow-wavelength OFDR analysis method, we calculated n_g versus wavelength for the 15 μm wide waveguides on both layers of Wafer 2, with a 20 nm wide spectral window, yielding average group indices of 1.5045 and 1.5131 for layer 1 and 2, respectively. The disparity of $8.6 * 10^{-3}$, suggests a difference in either core geometry or refractive index.

Previous work on this Nitride-strip technology in [1] showed that thick deposited PECVD SiO_2 significantly reduces the refractive index of the Si_3N_4 core through the stress-optic effect, which provides a mechanism for deviation of the core refractive indices from those indicated in Table I. Additionally, Schriemer & Cada show in [6] that deposited upper cladding is the principal contributor to birefringence in planar waveguides, and Klein & Miller show that these stressy films create a vertically varying stress [7].

Therefore, it stands to reason that WG1 experiences a different stress than WG2 due to the vertical stress-gradient created by the upper cladding oxide, which produces a different refractive index in each waveguide plane. Waveguide modes simulated with finite difference showed that core indices of approximately 1.925 and 1.975 were needed to match the measured n_g values of layer 1 and 2, respectively, showing a significant index reduction in the lower layer. This will play a role in the mode coupling of a vertical directional coupler.

B. Vertical Coupling Loss

We determined the loss of the vertical directional couplers independently of the coupling ratio and propagation loss using a large array of vertical couplers with varying parameters. The fabricated array consisted of 11 directional couplers, each with varying coupling length from 0 μm to 500 μm, along with non-coupling reference waveguides on each layer. This set was repeated 8 times with a varying lateral offset from -1 μm to $+1$ μm in steps of 0.25 μm. Four of these eight sets were measured on the 4 μm wide guides of Wafer 1, corresponding to lateral offsets of -1.0, -0.25, 0.0 and $+0.25$ μm, for a total of 39 coupler (156 cross and bar) measurements and 8 reference waveguides (four on each layer). Polarization was optimized for TE mode excitation by observing 1550 nm laser throughput of the reference guides with an infrared camera, using a polarizing beam splitter to differentiate the TE & TM modes.

Coupling loss was calculated as the excess loss of the couplers with respect to the reference waveguides. For launch into a single input waveguide of a given coupler, this is calculated by subtracting the power throughput of the reference guides from the sum of both coupler outputs. We calculated an average coupling loss of 0.19 ± 0.20 dB, where the error from fiber coupling was reduced by the large number of

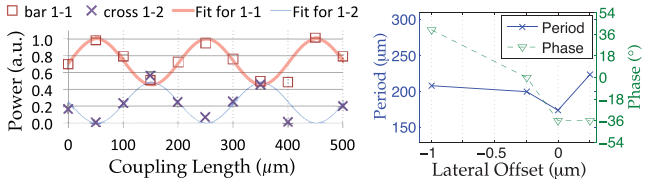

(a) (b)

Fig. 3. (a) Transmitted power (normalized) versus coupling length for launch into input #1 to cross (in 1→ out 2) and bar (in 1→ out 1) ports for the −0.25-μm lateral offset; one of the four measured on Wafer 1. (b) Fitted sinusoid period and phase for each lateral offset measured.

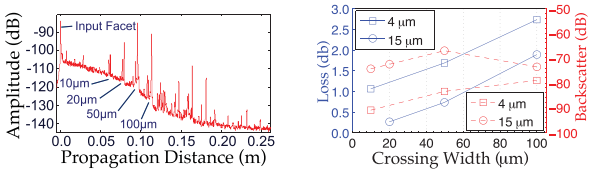

(a) (b)

Fig. 4. (a) OFDR of the spiral with crossing locations and widths indicated for the 15 μm × 60 nm guides on Wafer 2. (b) Losses (solid) and mode-coupled backscatter (dashed) incurred at each crossing width for the same.

measurements performed. Fig. 3(a) shows coupling data for one of the measured lateral offsets with sinusoidal fits overlaid.

Coupling amplitudes of less than 100% indicate that the two parallel waveguide layers are velocity mismatched, a direct result of the stress-related shift in modal indices shown in Section III-A and described in [8]. Maximum coupling was calculated as the largest percentage of power that leaves the 1→ 1 bar waveguide, with results of 54.0%, 54.7%, 48.8% and 50.0% for the −1.00, −0.25, 0.00 and +0.25 μm offsets, respectively. The phase increase with larger lateral offset in Fig. 3(b) suggests increased coupling in the waveguide bends, while the periodicity indicates that zero offset had the smallest coupling length, as designed.

C. Layer Interactions

Figure 4(a) shows the power versus distance into the multimode spiral with crossings on Wafer 2 (15 μm × 60 nm cores), where the data was acquired via OFDR and smoothed with a moving-window average. A reflection and drop in power is seen at each crossing, with both the reflection magnitude and transmission loss increasing with crossing width, as one would expect. Loss incurred by each crossing width was calculated by subtracting the reflection amplitude after the crossing from that before the crossing, and then correcting for the propagation loss incurred over that distance. This value was then halved to account for the double-pass of reflected light. We additionally calculate the power scattered into backward-propagating waveguide modes by integrating over each reflection peak.

The losses incurred by each crossing width are plotted in Figure 4(b), for both waveguide widths on Wafer 2. The propagation losses used to correct these values were between 21.2 dB/m and 31.3 dB/m. Interestingly, for the 15 μm wide guide, the 10 μm wide crossing incurs too little loss to differentiate from the propagation loss and measurement error, which indicates that it is well below 0.254 dB. Higher crossing losses for the 4 μm wide guides are a result of reduced modal confinement, causing a larger field overlap with layer WG2, with a minimum loss of 1.05 dB for the 10 μm wide crossing.

IV. Conclusion

We have fabricated vertically separated Si_3N_4 waveguide layers using standard PECVD depositions, in a platform similar to that used in our previously reported ultra-low loss technology. We probed the interactions between waveguides on adjacent layers in parallel and perpendicular orientations via vertical directional couplers and spirals with crossings, respectively.

Narrow-band OFDR with a 20 nm wide window revealed that film-stress plays a larger role than anticipated by altering the group indices of the two parallel waveguide planes by 8.6E-3. This consequently reduced the coupling coefficient of the vertical directional couplers, resulting in a maximum cross-coupling of 54.7%. The excess loss of the couplers is shown to be as low as 0.19 ± 0.20 dB for a 4 μm × 50 nm geometry. The stress-optic effect must be addressed with modal index compensation in the waveguide design, or via wafer bonded cladding oxide to reduce the induced stress.

Lastly, we show that for perpendicular crossings on adjacent layers, transmission loss is lower than 0.25 dB for the multimode 15 μm × 60 nm waveguide structure. For the single-mode 4 μm × 60 nm geometry, the minimum crossing loss is higher, at 1.0 dB for a 10 μm wide crossing. For the intended application of two overlapped spirals, the waveguides on adjacent layers will intersect at an angle. The directional couplers and perpendicular crossings investigated here represent the two extremes of 0° and 90°, respectively.

These results show the feasibility of overlapped waveguide layers for long delays, with low coupling losses for the single-mode designs and low crossing loss for the multimode design, while illustrating the necessity of film stress management.

Acknowledgment

The authors would like to thank S. Rodgers for supporting this work and useful discussions.

References

[1] J. F. Bauters, *et al.*, "Planar waveguides with less than 0.1 dB/m propagation loss fabricated with wafer bonding," *Opt. Express*, vol. 19, no. 24, pp. 24090–24101, Nov. 2011.

[2] J. F. Bauters, *et al.*, "Ultralow loss high-aspect-ratio Si_3N_4 wavequides," *Opt. Express*, vol. 19, no. 4, pp. 3163–3174, Feb. 2011.

[3] M. N. Armenise, C. Ciminelli, F. Dell'Olio, and V. M. N. Passaro, *Advances in Gyroscope Technologies*. New York: Springer-Verlag, 2010, pp. 32–27.

[4] B. E. Little, S. T. Chu, W. Pan, D. Ripin, T. Kaneko, Y. Kokubun, and E. Ippen, "Vertically coupled glass microring resonator channel dropping filters," *IEEE Photon. Technol. Lett.*, vol. 11, no. 2, pp. 215–217, Feb. 1999.

[5] Y. Kokubun, S. Kubota, and S. T. Chu, "Polarization-independent vertically coupled microring resonator filter," *Electron. Lett.*, vol. 37, no. 2, pp. 90–92, Jan. 2001.

[6] H. P. Schriemer and M. Cada, "Modal birefringence and power density distribution in strained buried-core square waveguides," *IEEE Quantum Electron.*, vol. 40, no. 8, pp. 1131–1139, Aug. 2004.

[7] C. Klein and R. Miller, "Strains and stresses in multilayered elastic structures: The case of chemically vapor-deposited ZnS/ZnSe laminates," *J. Appl. Phys.*, vol. 87, no. 5, pp. 2265–2272, Mar. 2000.

[8] L. A. Coldren and S. W. Corzine, *Diode Lasers and Photonic Integrated Circuits*. New York: Wiley, 1995.